Plasma Chemical Vapor Deposition of TiB_2†

Fukuhisa MATSUDA*, Kazuhiro NAKATA and Takeshi OHTSUBO*****

Abstract

Low temperature deposition of TiB_2 has been investigated by means of a direct current discharge type plasma assisted CVD process in $TiCl_4+BCl_3+H_2$ reactant gas system on the molybdenum sheet as a substrate.

TiB_2 film was deposited on Mo substrate at 773K for the wide gas flowrate ratio of $BCl_3/TiCl_4$, r, ranging from 1.0 to 10 under the condition of total gas pressure: 133Pa, gas flowrate of $TiCl_4$: 10SCCM and H_2: 800SCCM. Especially, for flowrate ratio of r=2 to 8, adhesive and dense TiB_2 film with almost stoichiometric composition was successfully deposited without no spalling and cracking. Film hardness and deposition rate were increased as the increase of flowrate ratio, r and maximum values of about Hv3500 and 4.5 μm/h, respectively were obtained at r=6 to 8.

KEY WORDS : (Plasma CVD) (TiB_2) (Molybdenum) (Film Deposition) (Deposition Rate) (Hardness) (Structure) (Composition)

1. Introduction

Titanium diboride(TiB_2) has many excellent properties such as high hardness, excellent resistances to wear, high temperature oxidation and corrosion in addition to good electric conductivity[1]. Therefore, TiB_2 coating is expected as an excellent protective coating on the materials used under severe wear and corrosive environments.

The synthesis of TiB_2 film has been made mainly by means of thermal CVD process by the $TiCl_4+BCl_3+H_2$ system the reactive temperature from 1023K to 1873K[2-14]. However, high reactive temperature hinders the wide application of TiB_2 coating because of the degradation of the substrate material or component.

On the contrary, It is well known that there are some low temperature deposition processes such as spattering, ion-plating and plasma CVD so on, and these processes are already utilized as an actual industrial deposition process, for example, for the deposition of TiN and TiC coatings. There are, however, few reports about low temperature TiB_2 deposition by spattering[15,16] and ion-plating[17], and almost no attempt was reported about TiB_2 deposition by plasma CVD.

The aim of this report is to make TiB_2 film at lower temperature, about 773K by emplying plasma CVD process in $TiCl_4+BCl_3+H_2$ system and to make clear the effect of process parameter, mainly molar ratio of B/Ti in reactant gases on the characteristics of deposited film, deposition rate, hardness, surface morphology, structure and composition.

2. Fundamental CVD Reaction of TiB_2

Overall reaction of CVD of TiB_2 in $TiCl_4+BCl_3+H_2$ system is written as follows:

$$TiCl_4+2BCl_3+5H_2 \rightarrow TiB_2+10HCl \quad (1)$$

T.M. Besmann and K.E. Spear[18] obtained Eq.(2) by the calculation from thermodynamic data,

$$\ln K=31.32-35330/T \quad (2)$$

where K is the equelibrium constant for Eq.(1) and T is the absolute temperature.

K is a constant defined by

$$K=\exp(-\Delta G^\circ/RT) \quad (3)$$

where ΔG° is the standard free energy change for Eq.(1), R is the ideal gas low constant.

From Eqs.(2) and (3), relationship between ΔG° and T for eq.(1) is obtained as Eq.(4), and is shown in **Fig.1**

$$\Delta G^\circ=70.20-0.06223T \quad (4)$$

From Eq.(4), reactive temperature more than 1128K is required to yield TiB_2 film in thermal CVD in $TiCl_4+BCl_3+H_2$ system.

It is, however, expected that this reactive temperature can be lowered less than 1128K in plasma assisted CVD

† Received on May 7, 1990

* Professor
** Instructor
*** Graduate Student, now with Showa Aluminum Corporation

Transactions of JWRI is published by Welding Research Institute of Osaka University, Ibaraki, Osaka 567, Japan

Table 1 Substrates used and their specimen sizes

Substrate (#1200)	Mo	(10"×30'×1.5'mm)
	SUS 304	(15"×30'×4.0'mm)
	OFC	(10"×30'×2.0'mm)

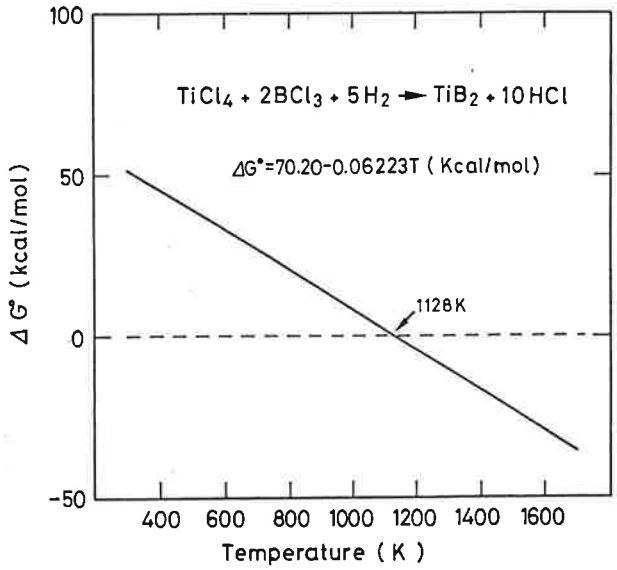

Fig. 1 Relation between temperature and free energy of TiB_2 formation.

process.

3. Materials Used and Experimental Procedures

3.1 Materials used

As substrate materials, molybdenum (Mo)sheet was mainly used and partly austenitic stainless steel SUS304 and oxygen free copper(OFC) plates were also used for comparison. **Table 1** shows the size of substrate specimen. Specimen was polished on its surface with emery paper(# 1200) and then ultrasonically cleaned in acetone bath prior to coating treatment.

3.2 Plasma CVD process and its apparatus used

Figure 2 shows the schematic diagram of the plasma CVD apparatus which consists of a reactive chamber, a power supply, a reactant gas supply and a vacuum unit. This apparatus is almost the same in fundamental system as the plasma ion nitriding apparatus[19].

Glow discharge plasma is generated by applying a DC voltage between a chamber wall as an anode and a specimen holder as a cathode. Substrate is put on the cathode and heated only by the glow discharge heating. No other heating device was utilized.

Liquid $TiCl_4$(purity 99.99%), hydrogen diluted BCl_3

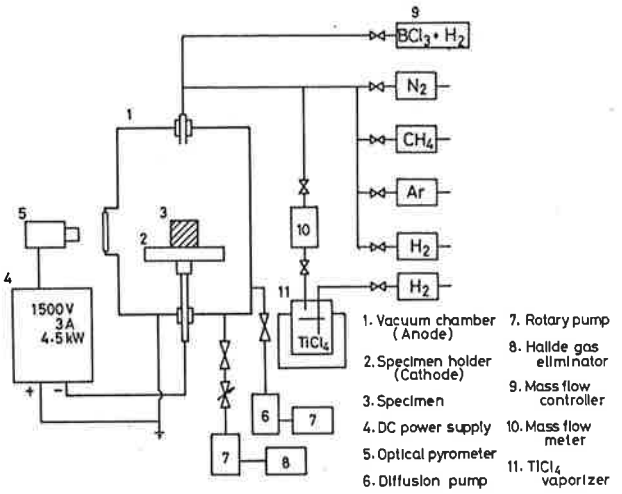

Fig. 2 Schematic illustration of the experimental apparatus for plasma CVD.

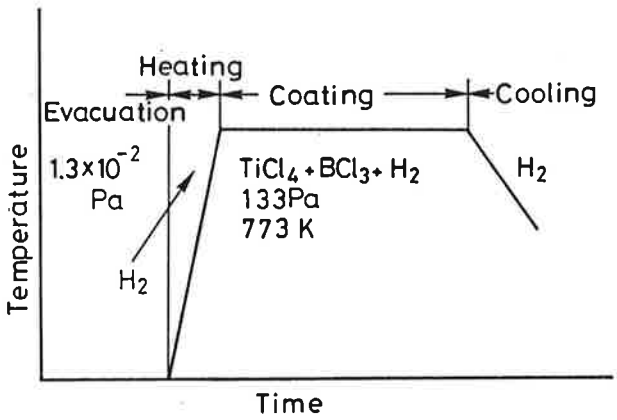

Fig. 3 Schematic diagram of thermal cycle for plasma CVD process used.

(10vol%BCl_3+H_2) and H_2(99.9999%) gases were used as source materials. $TiCl_4$ was supplied from a special vaparizer hold at 293k by using H_2 gas as a bubbling and carrier gases. Flowrate of these gases were controlled by the mass flow controllers. Treating temperature was measured with a optical pyrometer on the surface of the substrate put on the cathode holder.

Figure 3 shows the schematic diagram of thermal cycle used for plasma CVD process in this study. After the evacuation to 1.3×10^{-2} Pa, H_2 gas was introduced to 133 Pa and glow discharge was started to heat the substrate to the treating temperature, and then reactant gases of $TiCl_4$ and BCl_3 were fed for TiB_2 deposition with a constant and a desired mixture ratios. After treatment, coated specimen was cooled in a furnace under H_2 gas atmosphere.

Treating temperature and total gas pressure were kept constant, 773K and 133 Pa, respectively. Flowrate ratio of

$BCl_3/TiCl_4$, r, was varied from 1 to 10 under constant $TiCl_4$ flowrate of 10SCCM and constant total H_2 flowrate of 800SCCM.

3.3 Characterization method of deposited film

Surface morphology and structure on the crosssection of the deposited film which was artificially fractured were observed by SEM, and at the same time film thickness was measured on the crosssection. Identification of deposited film and its composition were carried out by using X-ray diffractometry (CuK α radiation), EPMA and X-ray photoelectron spectroscopy.

Hardness measurement of deposited film was carried out on its surface by Vickers hardness tester with 0.98N load.

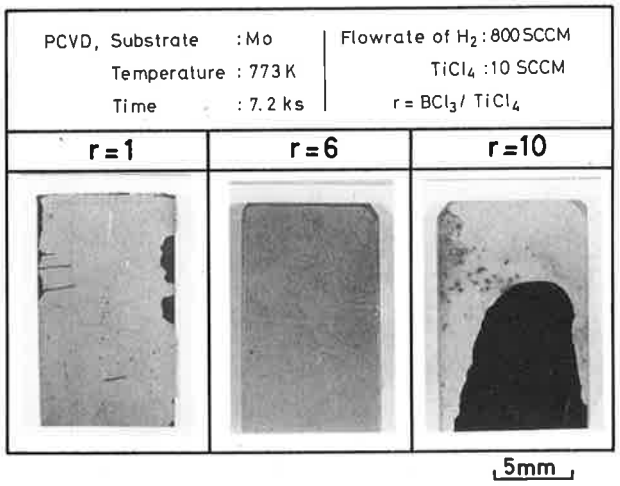

Fig. 4 Appearance of specimen after plasma CVD coating on Mo substrate (Peeled part appeares black)

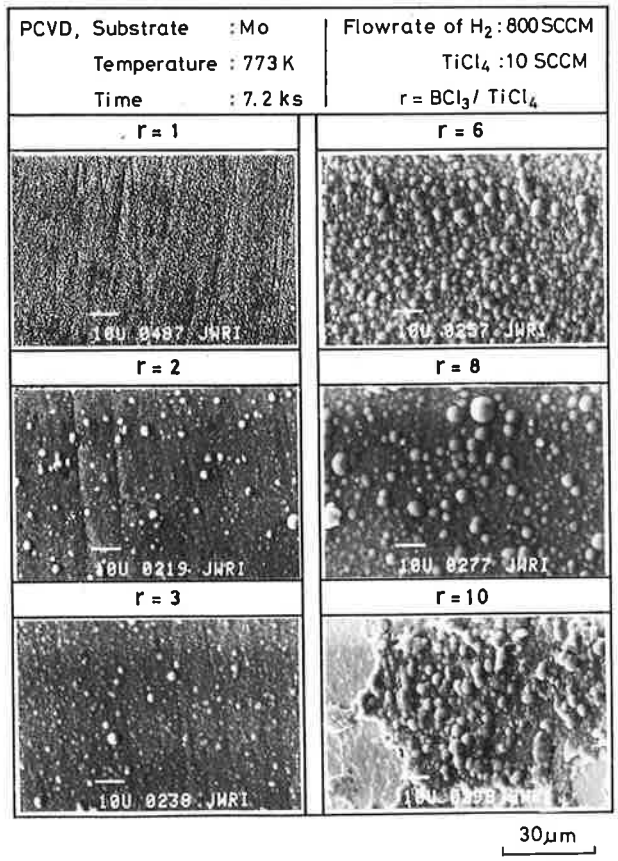

Fig. 5 Surface morphology of deposited film on Mo substrate at different $BCl_3/TiCl_4$ flowrate ratio,r observed by SEM.

4. Results and Discussions

4.1 Morphology

Figure 4 shows the typical appearance of coated specimen of Mo substrate at r = 1,6 and 10. A light gray film was deposited at each condition, but peeling of film from Mo substrate was observed at r = 1 and 10, especially it was much severe at r = 10. However no peeling was observed at other conditions of r = 2 to 8 as same as r = 6 in Fig.4.

Figures 5 and 6 show the typical surface and cross-sectional structures revealed by SEM for deposited films obtained at different gas flowrate, r.

In Fig.5, very smooth surface with fine spherical deposits was observed at r = 1. However, large spherical

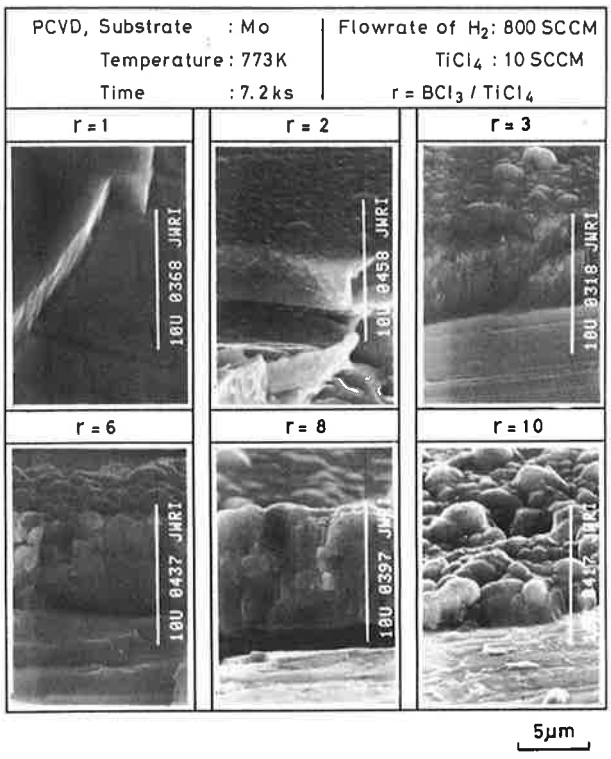

Fig. 6 Crosssectional micrograph of TiB_2 films deposited on Mo substrate at defferent $BCl_3/TiCl_4$ flowrate ratio,r observed by SEM.

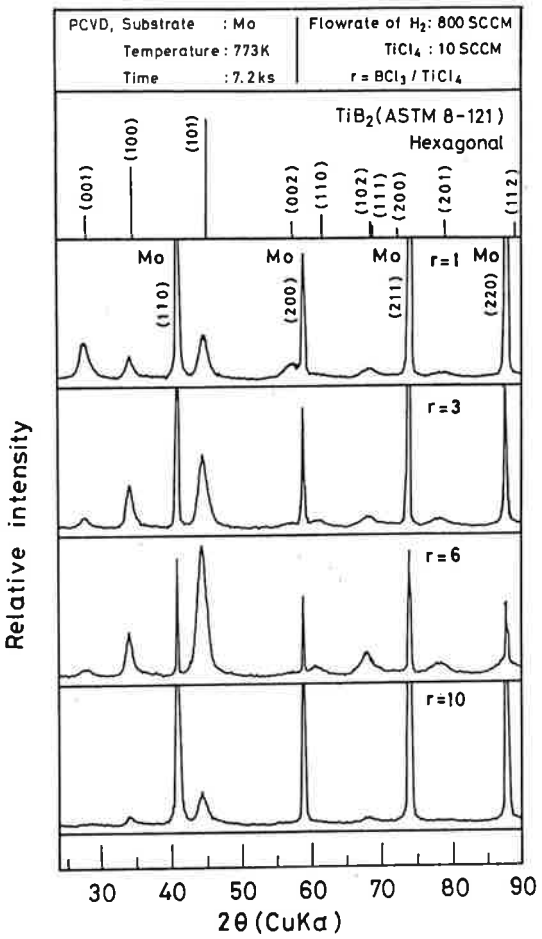

Fig. 7 Typical X-ray diffraction pattern of TiB_2 films deposited on Mo substrate at different $BCl_3/TiCl_4$ flowrate ratio,r.

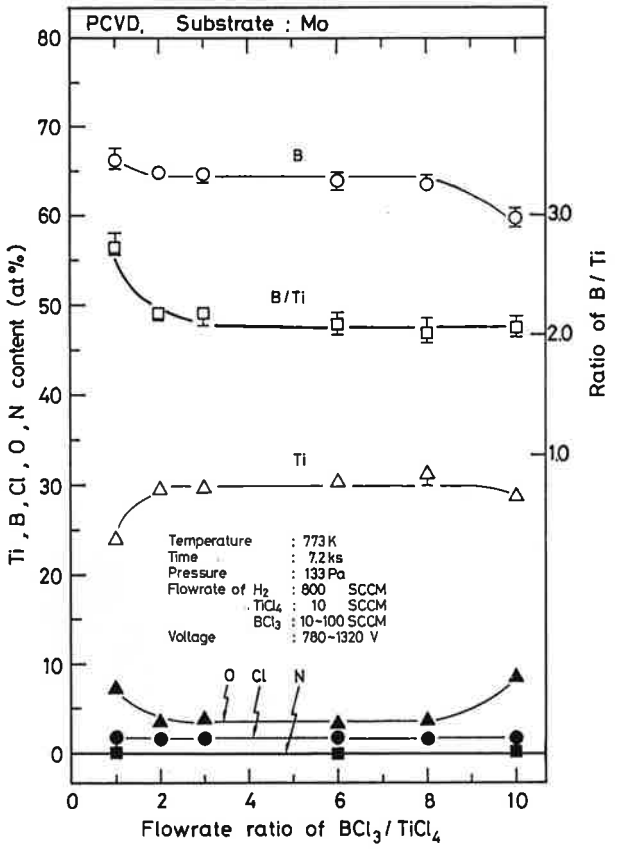

Fig. 8 Effect of $BCl_3/TiCl_4$ flowrate ratio,r on Ti,B,Cl,O and N contens in TiB_2 film measured by EPMA.

deposits began to appeare at r=2. The number and size of these large spherical deposits were increased as the increase of r and film surface was almost covered with them at more than r=6.

These surface structure coincided with the cross-sectional structure as shown in Fig.6. That is, the fractured surface of coated films at r=1 was very smooth and no grain structure was observed. At r=2, the film consisted of fine and dense equiaxed grain structures. On the contrary, columnar grain structure was begun to be observed at more than r=3 and columnar grains became coarse with the increase in flowrate ratio,r, though grain structure became irregular at r=10.

4.2 Results of X-ray diffraction analysis

Figure 7 shows the typical X-ray diffraction pattern obtained from the surface of the film deposited on Mo substrate at different $BCl_3/TiCl_4$ flowrate ratio,r.

Besides the sharp and strong peaks from Mo substrate, only the peaks of hexagonal type TiB_2 were observed. Other phases which appeared in Ti-B binary system of equilibrium phase diagram[20], that is, boron and other titanium boride, Ti_3B_4 and TiB were not detected.

Crystalline orientation of the deposited film were similar to that from powder material(ASTM 8-121) shown in upper zone in Fig.7 except for r=1 where (001) peak was relatively strong. As the increase of r, (001) peak was lowered and on the contrary, (101) peak became stronger, especially at r=6.

It seems that these patterns are closely related to the film structure on its crosssection. That is, at r=1, mainly (001) plane of hexagonal structure was parallel to the substrate surface,i.e., c-axis was perpendicular to the substrate surface and in this case the crosssectional structure was smooth in its surface, not a columnar structure. Judying from the X-ray pattern at r=6 where columnar structure was well developed, these columnar structures were mainly composed of a crystal structure of which (101) plane was parallel to the substrate surface.

4.3 Composition of deposited film

Figure 8 shows the EPMA results of TiB_2 films deposited on Mo substrate with different $BCl_3/TiCl_4$ gas flowrate ratio,r.

Besides Ti and B, oxygen(O) and chlorine(Cl) were also contained as impurities, but nitrogen(N) was little contained, less than 0.1 at%. In addition, Mo from

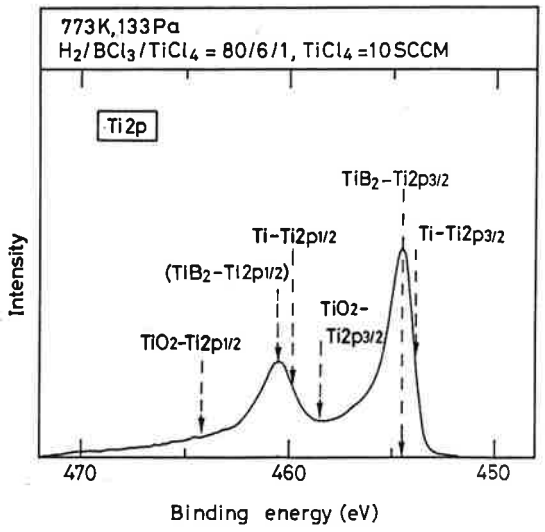

(a) Ti2p

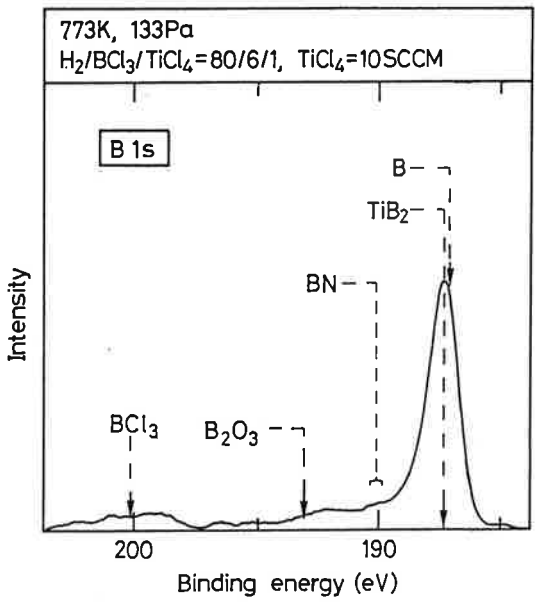

(b) B1s.

Fig. 9 Ti2p and B1s XPS spectra of TiB_2 film deposited at $BCl_3/TiCl_4$ flowrate ratio, r=6.

substrate was not detected in deposited film. These tendencies were almost equal at all of the r values in this study.

The ratio of B to Ti contents, B/Ti in deposited film was almost constant, 2.02 to 2.15 xecept at r=1 even for the wide range of gas flowrate ratio from r = 2 to 10. These B/Ti values were slightly higer, but almost equal to that of stoichiometric ratio of TiB_2, that is 2.0. However, at r = 1, B/Ti ratio in deposited film was exceptionally increased to about 2.7 because of lower Ti and higher B contents than those of the other gas flowrate ratio,r.

Cl content in deposited film was almost constant, about 1.7 to 2.0 at% for each r value. In CVD process

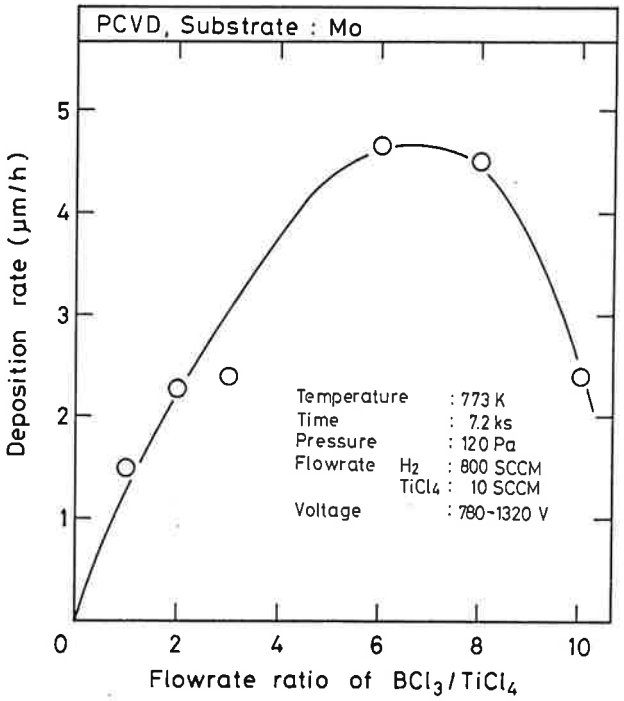

Fig. 10 Effect of $BCl_3/TiCl_4$ flowrate ratio,r on deposition rate of TiB_2 film.

which use the chloride as the reactant gas, the mixture of chlorine into the deposited film is inevitable at lower reaction temperature especially with plasma CVD process as reported, for example in TiN deposition[21].

O content was also constant, 3.3 to 3.9 at% for r=2 to 8, but it became higher at r=1 and 10, that is, 7.3 to 8.5 at%. In this study high purity reactant gas was used, so, the origin of oxygen was seemed to the adsorbed water and resedual gases in chamber wall.

Figure 9(a) and **(b)** shows the typical X-ray photoelectron spectra of deposited films at flowrate ratio, r=6. The binding energies[22] of Ti2p and Bls coincided to those of TiB_2, that is, 454.5eV for Ti2p3/2 and 187.3eV for Bls, respectively. However, as B1s of amorphous boron is 187.1eV, quite near to that of TiB_2, it was difficult to decide the presence of amorphous boron in deposited film. Moreover, as shown in **Fig.9(a)**, TiO_2(459.1 and 464.8eV for Ti2p3/2 and Ti2p1/2, respectively) was not detected.

Some other broad subpeaks besides TiB_2 were observed in Bls spectrum in Fig.9(b). BN(90.1eV), B_2O_3 (191.3eV) and BCl_3(200.5eV) were located near these subpeaks. EPMA results showing the mixture of O and Cl in deposited film suggested the formation of these oxide and chloride, but their presences were not clear, because these subpeaks in XPS spectrum were very weak.

In addition, almost the some XPS spectra as shown in Fig.9 were obtained at all of the other different r values.

4.4 Deposition rate

Figure 10 shows the effect of flowrate ratio on the deposition rate of TiB_2 film on Mo substrate. Deposition rate was almost linearly increased as the increase of flowrate ratio, r up to r=6 and it reached maximum value of about 4.5 μm/h at r=6 to 8.

However, abrupt decrease in deposition rate was observed at r = 10. The increase of BCl_3 flowrate caused the increase in total amount of Cl in reactant atmosphere, but in this study total flowrate of H_2 was kept constant, 800SCCM. Therefore furthermore excess of BCl_3 caused the unsufficient reduction of Cl by H_2 and this may disturb the TiB_2 deposition.

In addition, similar relationship between deposition rate and flowrate ratio was reported in TiB_2 deposition by thermal CVD process, though maximum deposition rate was obtained at r = 2 to 3[9,10]. Therefore this result means that effective molar B/Ti ratio in reactant gas in plasma CVD process is much larger than that in thermal CVD process.

It is generally known that in plasma CVD process, reactant gases introduced into plasma zone are decomposed to make many kinds of radical species, such as ions and activated neutral species and among them only limited radical species can react to form the objective product. Therefore, at the same time, many biproducts are also yielded in general in plasma CVD process and most of them are deposited on a chamber wall or otherwise exhausted to vacuum pump.

Therefore, it is considered that the most effective gas flowrate ratio in plasma CVD process does not always coincide with that for thermal CVD process.

It seems to depend on the ratio of the effective Ti and B species existing in plasma, though the kind of these species were not investigated in this study.

4.5 Hardness

Figure 11 shows the effect of flowrate ratio of $BCl_3/TiCl_4$, r, on the surface hardness of TiB_2 films deposited on Mo substrate.

Surface hardness of TiB_2 film was increased as the increase of r except for r=1 and reached maximum value of about Hv3500 at r = 6 to 8, though scattering in hardness at r = 8 was large because of its surface roughness. This hardness value is equal to those reported as TiB_2 balk material of Hv3370[1]. However, at r = 10, surface hardness was abruptly decreased to about Hv500.

The lower hardness values under r=6 and over r=10 are considered to be due to relatively thin film thickness. However, at r=1 its hardness was abnormally high even that its film thickness was the thinnest. This is due to its crystalline structure showing the preferred orientation of (001), of which c-axis was perpendicular to the substrate surface.

4.6 Influence of plasma discharge characteristics

The variations in discharge voltage and current against the gas flowrate ratio,r, are shown in **Fig.12** under the

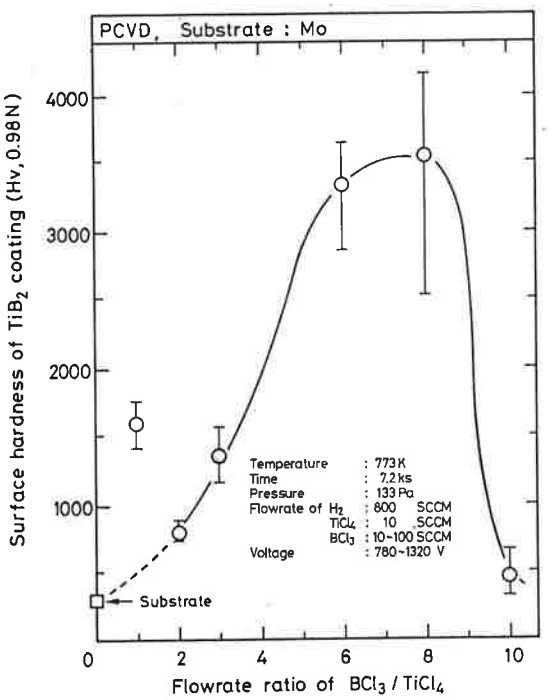

Fig. 11 Effect of $BCl_3/TiCl_4$ flowrate ratio,r on surface hardness of TiB_2 film.

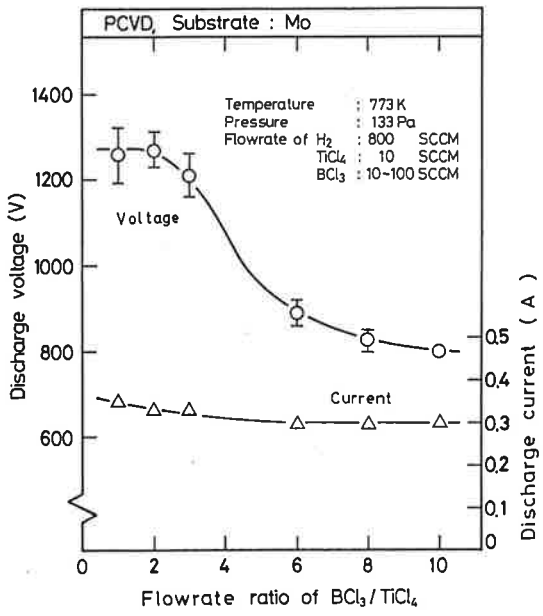

Fig. 12 Effect of $BCl_3/TiCl_4$ flowrate ratio,r on discharge voltage and current at constant substrate temperature of 773K.

condition where specimen temperature was kept constant by changing the discharge input.

At lower flowrate ratio less than r = 3, discharge voltage was high, about 1200 to 1300V. However, more increase in flowrate ratio decreased the discharge voltage abruptly to about 800V.

On the contrary, variation of discharge current was small and only a slight decrease was observed as the increase in flowrate ratio.

These results indicates that BCl_3 gas is easy to be ionized.

On the other hand, these variations in discharge voltage against flowrate ratio,r, is expected to affect the deposition rate and the structure of the deposited film. In DC plasma CVD process, the surface of depositing film is simulutaniously subjected to ion spattering during discharge process. Therefore, observed deposition rate is the sum of actual deposition rate by plasma chemical reaction and the errosion rate by ion spattering.

It is well known that ion spattering become harder as the increase in discharge voltage. Therefore, according to above idea, it seems that the increase in flowrate ratio causes the increase in deposition rate by decreasing the discharge voltage as shown in **Fig.13** which indicating the relation between deposition rate of TiB_2 film and discharge voltage.

On the other hand, hard ion spattering due to high discharge voltage also affect the film structure to restrict the film growth and this may cause the formation of smooth surface and fine grain structure. These tendencies coincided with structural change observed against the variation of flowrate ratio as shown in Figs.5 and 6.

That is to say, at low flowrate ratio with high discharge voltage, deposition rate was low and smooth surface and fine structure of film was obtained. On the contrary, at high flowrate ratio, as the decrease in discharge voltage, deposition rate was increased and the surface morphology and the structure became rough and coarse, respectively, except for r=10.

Concequently, it is considered that variation of deposition rate and the structure morphology of deposited TiB_2 film were affected not only the gas flowrate ratio itself but also the variation of discharge voltage caused by the variation of flowrate ratio.

4.7 Deposition on different kind of substrate material

Figure 14 shows the appearances of TiB_2 films deposited on different kinds of substrate material, Mo, SUS304 and Cu(OFC) at the optimum treating condition of r = 6. In addition **Table 2** shows the linear thermal expansion coefficient of these materials in comparison with TiB_2. Mo has almost the same thermal expansion coefficient of TiB_2, but those of SUS304 and Cu are much larger than TiB_2.

There was no cracking and peeling in deposited film on

Table 2 Linear thermal expansion coefficients of TiB_2, Mo, SUS304 and Cu.

	Linear thermal expansion Coefficient, α ($\times 10^{-6}$/K)
TiB_2	7.9
Mo	5.7 (293 ~ 773 K)
SUS304	18.4 (273 ~ 811 K)
Cu(OFC)	18.3 (273 ~ 773 K)

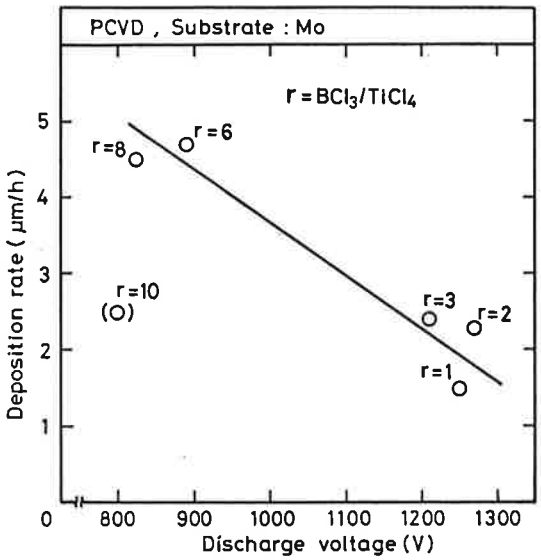

Fig. 13 Relation between discharge voltage and deposition rate of TiB_2 film.

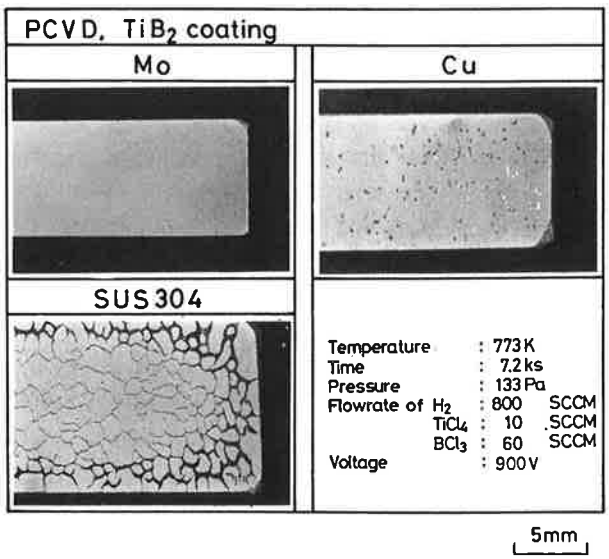

Fig. 14 Difference in surface morphology of TiB_2 film deposited on different substrate materials.

Mo substrate. Cu specimen was deformed after film deposition as the deposited side surface was tensioned and the opposite side was compressive because the linear thermal expansion coefficient of Cu was much larger than that of TiB_2. This caused many thin crackings perpendicular to tensile strain direction and partly spotted peeling was also observed associated to these cracking, though adhesion between film and Cu substrate was comparably good as same as Mo substrate in comparison with SUS304.

On the contrary, for SUS304 substrate, severe cracking with tortoiseshell-like morphology was occurred on its whole surface. The difficulty of TiB_2 deposition on ferromaterial by CVD process was also reported[4,23] and the reason was considered to be the errosion of substrate surface by the formation of $FeCl_2$[23]. This seems to cause the poor adhesion between TiB_2 film and substrate and promote the peeling of film incorporated with compreassive stress which may occur due to much large thermal expansion coefficient of substrate.

5. Conclusions

Low temperature deposition of TiB_2 film was studies by DC glow discharge type plasma CVD process and effect of its process parameter on the characteristics of deposited film has been investigated.

Main conclusions obtained in this study are as follows:

1) TiB_2 film was deposited on molybdenum substrate at 773K for the wide flowrate ratio of $BCl_3/TiCl_4$, r, ranging from 1.0 to 10 under the condition of total gas pressure of 133Pa, flowrate of $TiCl_4$ of 10SCCM and H_2 of 800SCCM.
2) The structure of the deposited film was monolithic and consisted of a hexagonal type TiB_2 with almost stoichometric composition except at r=1.
3) At flowrate ratio, r=2 to 8, adhesive and dense TiB_2 film was successfully deposited on molybdenum substrate without no spalling and cracking. At r=1 and 10, slight and severe spalling and cracking occurred, respectively.
4) Surface hardness and deposition rate of TiB_2 film were increased as the increase of flowrate ratio, r, and their maximum values of about Hv3500 and 4.5 μm/h, respectively were obtained at r=6 to 8. More increase than r=10 caused the abrupt decrease in surface hardness and deposition rate. Surface hardness depended mainly on the film thickness except at r=1.
5) Morphology of TiB_2 film was changed from smooth surface with dense and fine grain structure at less than r=3 to rough surface with coarse columnar grain structure as the increase of flowrate ratio,r.
6) As to the kind of substrate, among molybdenum, copper and austenitic stainless steel SUS304, adhesive TiB_2 deposition was obtained only on molybdenum. Cracking and spalling in deposited film occurred on the other substrates.

Acknowledgement

The authors would like to express their thanks to Mr. Masahiro Satoh, Osaka Prefectural Industrial Technology Research Institute for XPS analysis and Mitsubishi Metal corporation for EPMA analysis and also Nippon Denshi kogyo Co.Ltd. for technical assistant about plasma CVD apparatus.

This research was supported by Grant-in-Aid for Scientific Research(A) from the Ministry of Education, Science and Culture of Japan.

References

1) P.A. Dearnley and T.Bell: Surface Engineering,1(1985), 203.
2) R.E. Gannon, R.C. Folweiler and T. Vasilos: J. Amer. Ceram. Soc., 46(1963), 496.
3) J.J. Gebhardt and R.F. Cree: J. Amer. Ceram. Soc., 48(1965), 262.
4) T.Takahashi and H.Kamiya: J. Crystal Growth, 26(1974), 203.
5) T.M. Besmann and K. E. Spear: J. Crystal Crowth, 31 (1975), 60.
6) H.O. Pierson and E. Randich: Proc. 6th Inter. Conf. on CVD, 1977, Electrochemical Soc., 304.
7) G.Blandenet et al: Proc.6th Inter. Conf. on CVD, 1977, Electrochemical Soc., 330.
8) L.R. Newkirk et al: Proc. 7th Inter. Conf. on CVD, 1979, Electrochemical Soc., 515.
9) F.Zeman et al: Proc. 8th Inter. Conf. on CVD, 1981, Electrochemical Soc., 628.
10) H.O. Person and A.W. Mullendore: Thin Solid Films, 95(1982), 99.
11) G. Auner, Y.F. Hsieh and K.R. Padmanabhan: Thin Solid Films, 107(1983), 191.
12) A.J. Caputo, W.J. Lackey and I.G. Wright: ORNL/TM-9042, 1984.
13) T.M. Besmann and K.E. Spear: J. Crystal Growth, 31 (1985), 60.
14) S. Motojima and H. Hotta: J. Less-Common Metals, 141 (1988), 327.
15) J.G. Ryan et al: Thin Solid Films, 153(1987), 329.
16) J.T. Prater: J. Materials for Energy systems, 8(1987), 420.
17) H. Nishida and H. Kawasaki: HYOMEN GIJUTSU, 40 (1989), 598(in Japanese).
18) T.M. Besmann and K.E. Spear: J. Electrochem. Soc., 124 (1977), 786.
19) F. Matsuda, K. Nakata and T. Tohmoto: Trans. JWRI, 12 (1983), 271.
20) T.B. Massalski(Edi.): Binary Alloy Phase Diagrams, Vol.1, 1986,ASM.
21) K. Oguri, H. Fujita and T. Arai: HYOMEN GIJUTSU, 40(1989), 539(in Japanese).
22) G.E. Mullenberg(Edi.): Handbook of X-ray Photoelectron Spectroscopy, 1979, Perkln-Elmer Cop.
23) R. Bonetti, D. Comte and H.E. Hinterman: Proc. 7th Inter. Conf. on CVD, 1975, Electrochemical Soc., 495.